

SEMICLASSICAL CALCULATIONS OF THE QUADRUPLY EXCITED FOUR-ELECTRON SYSTEMS

N. Simonović¹, M. Predojević², V. Panković² and P. Grujić¹

¹*Institute of Physics, P.O. Box 57, 11000 Belgrade, Serbia*

²*Gymnasium, Trg Pobede 2a, 22320 Indjija, Serbia*

(Received: May 24, 2007; Accepted: June 18, 2007)

SUMMARY: Highly excited atoms acquire very large dimensions and can be present only in a very rarified gas medium, such as the interstellar space. Multiply excited beryllium-like systems, when excited to large principal quantum numbers, have a radius of $r \sim 10 \mu$. We examine the semiclassical spectrum of quadruply highly excited four-electron atomic systems for the plane model of equivalent electrons. The energy of the system consists of rotational and vibrational modes within the almost circular orbit approximation, as used in a previous calculation for the triply excited three-electron systems. Here we present numerical results for the beryllium atom. The lifetimes of the semiclassical states are estimated via the corresponding Lyapunov exponents. The vibrational modes relative contribution to the energy levels rises with the degree of the Coulombic excitation. The relevance of the results is discussed both from the observational and heuristic point of view.

Key words. ISM: atoms – **Methods:** analytical

1. INTRODUCTION

Quantum mechanical description of atomic structure has been successfully applied for not highly excited few-electron systems. However, as the degree of excitations increases direct application of the quantum mechanical formalism becomes cumbersome (see e.g. Bao 1993, 1994), due to a strong mixing of many states (e.g. Nicolaides et al. 1993, Kominos and Nicolaides 1994) and semiclassical calculations turn out more feasible. (For the triply excited lithium see the recent comprehensive review by Madsen (2003)). Semiclassical models appear particularly suitable for those few-electron configurations which possess a high degree of spatial symmetry (e.g. Grujić 1999). As the quantum mechanical calculations have shown, these symmetrical configurations are gradually attained as the degree of excitation,

characterized by the principal quantum number n , rises. In the case of the intrashell quadruple excitations ($2 \leq n \leq 6$), the electrons tend to acquire positions at the vertices of a tetrahedron and a simple Rydberg formula provides a plausible estimate of the energy spectrum (Kominos and Nicolaides 1994). Recent calculations by Poulsen and Madsen (2005a, 2005b) and Morishita and Lin (2005) confirm that the tetrahedral configuration describes reasonably well a number of low-lying quadruply excited states.

Multiply excited atoms have been reported under laboratory conditions, but only for the low degree of excitation, as with recent results by Hasegawa et al. (2006) on the multiple photo-excitation of beryllium by the synchrotron radiation. The so called hollow atoms with configurations ($2s^2 2p 3s$) (double excitation) and ($1s 3s^2 3p$) (triple excitation) have been produced.

Highly excited few-electron states belong to the so called small energy system case. They can be achieved by the near-threshold collisional processes (Simonović and Grujić 1996, Kuchiev and Ostrovsky 1998) or by synchrotron radiation photo-excitations. In the former case small-energy electrons tend to exchange their angular momenta and acquire very high values of the latter, even if the total angular momentum is small. On the other hand, photo-ionization may result in the total high angular momentum of the system in its final states. Another process that may result in highly multiply excited states is the electron capture via the charge-exchange collisions in plasma. For the classical configurations with single electron, orbital momenta quantum numbers high and close to their maximum values, electron paths are well approximated by circular orbits. These orbits turn out unstable, and this corresponds to the metastable quantum states. By applying standard semiclassical quantization rules, one can evaluate rovibronic energy spectra, as was done for two and three-electron multiply excited systems (Grujić 1988, 1999). Further, by evaluating the corresponding Lyapunov exponents, a lifetime of these periodic orbits can be estimated (Cvejanović *et al.* 1990).

In the recent paper the quadruple excitation of beryllium has been examined within a semiclassical model (Simonović and Grujić 2007). Apart from making use of the Newtonian formalism instead of the Hamiltonian one, the present calculations differ from those in a number of other respects. First, we deal here with very highly excited states, which allows a number of approximations to be made. The first of them is neglecting of the inertial effect, which appear via Coriolis force. Second, we employ the quantization rules appropriate to the Coulombic systems, rather than to the rotor-like objects. By neglecting weak couplings between different mode-subspaces, we are able to evaluate approximately the ro-vibronic spectrum for the highly excited states.

The general procedure for calculating semiclassical energies and lifetimes is as follows. One first finds periodic classical orbits and then applies standard quantization rules to quantize the energy spectrum. In the next section we quote two of possible classical models and carry out calculations for the plane configuration. In section 3 the energy spectrum of the beryllium atom is evaluated and in the last section we discuss the results and feasibility of their experimental verifications.

2. THE SEMICLASSICAL MODELS

Similarly to the continuum states, the first step in establishing the classical model is to set up the skeleton, equilibrium configuration, which corresponds to the so called leading (scaling) configurations in the near-threshold regime. In the planar case there is a strong analogy between the bound and continuum states symmetry, as in the case with the three electron system (Grujić 1999). However, moving to three dimensional configuration this analogy is partially lifted. Namely, the central symmetry

present in the free motion case goes into a more restricted symmetry for the bound motion. This is a direct consequence of the change of the active degrees of freedom. In the near-threshold kinematics the main direction is the radial one, whereas for the negative energy states it is the angular motion that supports the bounded motion. In determining the skeleton configuration, one first establishes the static one and then finds dynamical equilibrium state. The most convenient way to examine few-body systems is to make use of the spherical collective coordinates, namely

$$\vartheta_{ij} = \angle(\vec{r}_i, \vec{r}_j) \quad - \quad \text{mutual angle}, \quad (1)$$

$$\alpha_{i1} = \arctan(r_i/r_1) \quad - \quad \text{hyperangle}, \quad (2)$$

where r_i are radial coordinates of the particles from the centre of mass of the entire system, and

$$R^2 = \sum r_i^2, \quad - \quad \text{hyperradius}. \quad (3)$$

Generally, to find the static skeleton configuration one calculates the minimum of the potential function

$$V(\alpha, \vartheta, R) = C(\alpha, \vartheta)/R, \quad (4)$$

on the hypersphere $R = R_0 = \text{const}$. In practice, one selects in advance obvious candidates with appropriate symmetry and then examines the corresponding potential functions. In the bounded motion case, the static equilibrium configuration may differ considerably from the kinematic skeleton, due to angular (transverse) motion, which is necessary to maintain the dynamic equilibrium.

We shall distinguish two classes of classical configurations, upon which one can apply semiclassical quantization. These are (i) large-amplitude oscillatory (see, e.g. Bao 1992) and (ii) rovibronic configurations. We examine here some rovibronic models with a high degree of symmetry. Our approach differs from the quantum mechanical models with a fixed radial coordinate, so called frozen- r approximation (see, e.g. Bao 1998). To emphasize the difference and in view of the later choice of the quantization procedure, it is in order to classify the models employed in our semiclassical calculations. More precisely, one must make a choice between Coulombic few-electron system paradigm and molecule-like models.

Because of the regular spacing of the electrons in the case of a symmetrical configuration, one may consider such systems as rigid bodies which preserve their shape within the kinematics they are subjected to. But this appearance is deceiving, for the Coulombic systems obey different dynamic laws as compared with the rigid bodies. For instance, a change in the angular velocity, resulting in the corresponding change of the angular momentum results in the change of the shape of the system. In the case of a purely rotational motion, this change means expanding or shrinking of the radial distances from the rotation axis. If we restrict ourselves to the angular momentum only, a change of its magnitude results

in new Keplerian orbits, for instance, with different eccentricities. Contrary to this, a rigid body, like a rigid rotator, preserves its shape, but changes its angular velocity. These quantitative differences in dynamical behaviour are well reflected in the quantization rules which are imposed to the rotating Coulombic and rotor-like systems.

Regular structures in the few-electron systems indicate correlated motions. These correlations are subjected to stable and unstable modes perturbations. The former are directed transversely to the electron radii, whereas the latter are along the radial coordinate. This sort of instability is absent from the molecule-like systems, which are based on different kind of interaction, like Morse potential. Generally, correlations transversely to the radii from the rotation axis are constructive, as opposed to those along the radial distance, which destroy the rotating structure. Within the context of the small-energy systems destructive correlations govern the near-threshold behaviour of a fragmentation function, and in the case of a quasi-bounded motion these instabilities determine the lifetime of the negative-energy systems.

Generally, making use of the molecule paradigm it is possible to extract a number of symmetry features useful for the classification of states (see, e.g. a recent paper by Walter et al. (2000)), but the attempts to push the analogy with the molecule paradigm too far did not fulfill early expectations (see, e.g. the recent papers by Madsen and Molmer (2001, 2002)).

2.1. Beryllium-like T1 model

We examine first the tetrahedron-like configuration subject to the rotation around one of its principal axes, which has S_2 symmetry (Landau and Lifshitz 1965), and which we designate as $T1$ model, as shown in Fig. 1. This model was investigated by Bao (1998) in the context of the quantum mechanical qualitative analysis of the low-lying intrashell states.

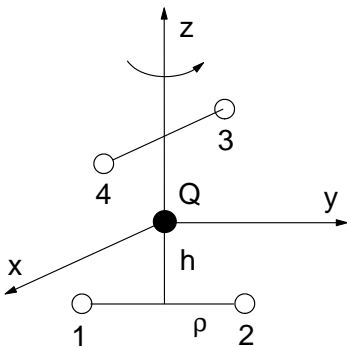


Fig. 1. Tetrahedron configuration skeleton model for the four-electron system.

By balancing Coulomb and centrifugal forces (zero radial force condition) one has (we use atomic units $\hbar = e = m_e = 1$, throughout)

$$\Omega^2 = \frac{1}{4\rho^3} - \frac{Q}{(\rho^2 + h^2)^{3/2}} + \frac{2}{[2(\rho^2 + 2h^2)]^{3/2}}, \quad (5)$$

where Ω is the angular velocity of the system and h the half-distance between the opposite sides along z -axis (see Fig. 1). From (5) one has

$$Q < \frac{(\rho^2 + h^2)^{3/2}}{2} \left[\frac{1}{2\rho^3} + \frac{\sqrt{2}}{(\rho^2 + 2h^2)^{3/2}} \right]. \quad (6)$$

From the requirement that the net Z (axial) component of the force which any of the four electrons experiences the $F_Z = 0$, one has

$$\frac{Qh}{(\rho^2 + h^2)^{3/2}} - \frac{\sqrt{2}h}{(\rho^2 + 2h^2)^{3/2}} = 0. \quad (7)$$

Apart from the trivial solution $h = 0$ (planar case), when the central charge must satisfy the inequality

$$Q > \frac{1}{4} + \frac{1}{\sqrt{2}}, \quad (8)$$

for the bound state to be possible (attractive centripetal force), for $h \neq 0$ from (7) one has

$$\frac{1}{2} < Q < \sqrt{2}, \quad (9)$$

that yields $Q = 1$ for the real atomic systems. Hence, it turns out that the model works only for H^{3-} anions, provided no further restrictions on Q are imposed.

2.2. Beryllium-like P1 model

This is an essentially planar quadratic configuration model, with the nucleus situated at the centre and electrons rotating around the axis perpendicular to the plane, as shown in Fig. 2. Oscillations around the skeleton equilibrium points (stable modes) are allowed, as well as radial deviations (unstable modes).

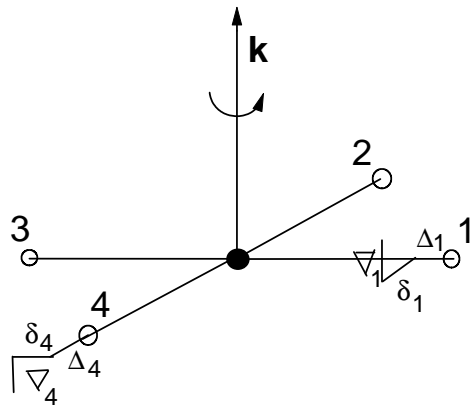


Fig. 2. Planar configuration four-electron rovibronic model.

3. ROVIBRONIC SPECTRUM

As stressed above we consider rovibronic motion as a superposition of rotational and vibrational motions of the equivalent electrons, without invoking the concept of a (rigid) rotor. We first find dynamic equilibrium configurations, by writing the corresponding Newton's equations for the electrons in the field of an infinitely heavy charge Q

$$\frac{d^2 \mathbf{r}_i}{dt^2} = \sum_{i \neq j} \frac{r_{ij}}{r_{ij}^3} - Q \frac{\mathbf{r}_i}{r_i^3}, \quad i \neq j = 1, 2, 3, 4. \quad (10)$$

These equations are then solved subject to the quantization condition

$$\mathcal{L} = L + \frac{1}{2}, \quad L = 0, 1, 2, \dots \quad (11)$$

where \mathcal{L} ($= 4\ell_e$) denotes the angular momentum of the entire system. This provides the third equation

$$\Omega = \frac{L + \frac{1}{2}}{4\rho^2}. \quad (12)$$

The semiclassical approximation applies for $L \gg 1$, and one obtains, in the zero approximation, a standard semiclassical spectrum (see e.g. Eqs. (4-9) in Grujić 1999)

$$E_L^{(0)} = -\frac{72 Q_{\text{eff}}^2}{(2L + 1)^2}, \quad (13)$$

with the effective charge given by

$$Q_{\text{eff}} = Q - \mu_{P1}, \quad \mu_{P1} = \frac{1}{\sqrt{2}} + \frac{1}{4} = 0.95711. \quad (14)$$

The screening parameter μ_{P1} is model dependent. Now, we allow for the small deviations from the skeleton configuration

$$\begin{aligned} \mathbf{r}_i &= (\rho + \Delta_i) \mathbf{n}_\rho^{(i)} + \delta_i \mathbf{n}_\phi^{(i)} + \nabla_i \mathbf{k}, \\ \Delta_i, \delta_i, \nabla_i &\ll r, \quad \mathbf{n}_\rho \perp \mathbf{n}_\phi \perp \mathbf{k}, \end{aligned} \quad (15)$$

where \mathbf{n} and \mathbf{k} are unit vectors in the corresponding directions. We consider the kinematics of small variations by inserting Eq. (15) into Newton's equations (10). In order to get corresponding equations it is convenient to pass to the comoving reference system, and neglect the coupling between the radial and tangential motions (Coriolis force). In this rotating frame ($\Omega' = 0$) we impose the following constraint

$$\mathbf{L}' = 0 \quad (\text{zero angular momentum}), \quad (16)$$

that gives

$$\nabla_1 = \nabla_3, \quad \nabla_2 = \nabla_4, \quad (17)$$

$$\delta_1 + \delta_2 + \delta_3 + \delta_4 = 0. \quad (18)$$

3.1. In-plane deviations

In Fig. 3 we show two possible oscillatory modes for the four-electron system. Since these decouple from those perpendicular to the skeleton (Oxy) plane, they are evaluated separately. Hyper-sphere constraints demand

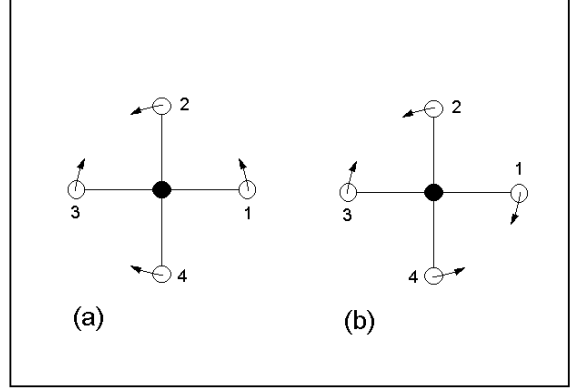


Fig. 3. Two possible vibration modes for the in-plane oscillations.

$$\sum_{i=1}^4 \mathbf{r}_i^2 \equiv R^2 = 4\rho^2, \quad (19)$$

providing

$$\Delta_1 + \Delta_2 + \Delta_3 + \Delta_4 = 0, \quad (20)$$

and this reduces the dimensionality of the system to 8. At fixed $r_i^{(0)} = \rho_i^{(0)}$, for the small deviations, one obtains the matrix equation (see Grujić 1983)

$$D^2 \mathcal{I} \mathbf{F} = \mathcal{B}^{(8)} \mathbf{F}, \quad D^2 \equiv r^3 \frac{d^2}{dt^2}, \quad (21)$$

where \mathcal{I} is the unit matrix, \mathbf{F} is the column vector

$$\mathbf{F} = \{\delta_1, \delta_2, \delta_3, \delta_4, \Delta_1, \Delta_2, \Delta_3, \Delta_4\}^T, \quad (22)$$

T denotes the row transposition, and

$$\mathcal{B}^{(8)} = \begin{pmatrix} a & 3b & \frac{1}{8} & 3b & 0 & b & 0 & -b \\ 3b & a & 3b & \frac{1}{8} & -b & 0 & b & 0 \\ \frac{1}{8} & 3b & a & 3b & 0 & -b & 0 & b \\ 3b & \frac{1}{8} & 3b & a & b & 0 & -b & 0 \\ 0 & -b & 0 & b & c & -3b & -\frac{1}{4} & -3b \\ b & 0 & -b & 0 & -3b & c & -3b & -\frac{1}{4} \\ 0 & b & 0 & -b & -\frac{1}{4} & -3b & c & -3b \\ -b & 0 & b & 0 & -3b & -\frac{1}{4} & -3b & c \end{pmatrix}, \quad (23)$$

with

$$a = \frac{1}{8}(1 - \sqrt{8}) - Q, \quad b = \frac{\sqrt{2}}{8}, \quad c = 2Q - \frac{1}{4}(1 + \sqrt{2}). \quad (24)$$

To solve (21), one can follow the standard procedure from the theory of small oscillations (see e.g. Simonović and Grujić 2007), which basically reduces to diagonalizing $\mathcal{B}^{(8)}$. The general solution of (21) consists then of a mixture of all possible frequencies of the modes present, for the harmonic and anti-harmonic motions around the corresponding equilibrium points. This rigorous procedure, however, conceals the underlying dynamics and the transparency of the physical picture is lost. We shall adopt, therefore, a different strategy in order to estimate the relevant eigenvalues and the associated proper frequencies (see later). We first evaluate radii of the electrons' circular paths, by balancing centripetal and centrifugal forces, taking into account quantization condition (11)

$$r_L = \frac{(2L+1)^2}{64Q_{\text{eff}}}. \quad (25)$$

3.2. In-plane vibrations

As we noted above, we avoid direct procedure of diagonalization of matrix $\mathcal{B}^{(8)}$ and consider Δ and δ subsystems from (21) separately, neglecting in (23) matrix elements which couple these two subspaces.

We start with the submatrix

$$\mathcal{B}_\delta^{(4)} = \begin{Bmatrix} a & 3b & \frac{1}{8} & 3b \\ 3b & a & 3b & \frac{1}{8} \\ \frac{1}{8} & 3b & a & 3b \\ 3b & \frac{1}{8} & 3b & a \end{Bmatrix}. \quad (26)$$

Making use of the constraint (17), matrix $\mathcal{B}_\delta^{(4)}$ is transformed into

$$\mathcal{B}_\delta^{(3)} = \begin{Bmatrix} a - 3b & 0 & \frac{1}{8} - 3b \\ 3b - \frac{1}{8} & a - \frac{1}{8} & 3b - \frac{1}{8} \\ \frac{1}{8} - 3b & 0 & a - 3b \end{Bmatrix}. \quad (27)$$

Generally, one proceeds by diagonalizing $\mathcal{B}_\delta^{(3)}$ as given by (27), but we shall adopt a shortcut for a simple estimate of the system vibrational motion. We impose further constraints on δ deviations, as the zero-order solution. Two types of the vibrational motion should be considered now.

(i) Electrons oppositely situated vibrate around the equilibrium positions in-phase, as shown in Fig. 3b. The constraints on δ are

$$\delta_1 = \delta_3, \quad \delta_2 = \delta_4, \quad \delta_1 = -\delta_2. \quad (28)$$

This reduces the matrix (27) to the scalar

$$\mathcal{B}_\delta^{(3)} = \lambda_\delta = a - 6b + \frac{1}{8} = \frac{1}{4} - \sqrt{2} - Q, \quad (29)$$

with the angular frequency

$$\omega_\delta^{(0)} = \frac{\eta_\delta^{(0)}}{(2L+1)^3}, \quad (30)$$

$$\eta_\delta^{(0)} = 512\sqrt{Q + \sqrt{2} - \frac{1}{4}} \left(Q - \frac{1}{4} - \frac{1}{\sqrt{2}}\right)^{3/2}. \quad (31)$$

(ii) Oppositely situated electrons run out-of-phase, Fig. 3a. The constraints read now

$$\delta_1 = -\delta_3, \quad \delta_2 = -\delta_4, \quad (32)$$

that yields for the diagonal elements

$$\lambda_\delta^{(-)} = -(Q + \frac{\sqrt{2}}{4}). \quad (33)$$

The corresponding frequency is given by

$$\omega_\delta^{(-)} = \frac{\sqrt{-\lambda_\delta^{(-)}}}{r_L^{3/2}}, \quad (34)$$

which provides finally

$$\omega_\delta^{(-)} = \frac{\eta_\delta^{(-)}}{(2L+1)^3}, \quad (35)$$

$$\eta_\delta^{(-)} = 512\sqrt{Q + \frac{\sqrt{2}}{4}} \left(Q - \frac{1}{4} - \frac{1}{\sqrt{2}}\right)^{3/2}. \quad (36)$$

Similarly, for the Δ subspace we shall adopt a shortcut for a rough estimate of the system instability:

$$\mathcal{B}_\Delta^{(4)} = \begin{Bmatrix} c & -3b & -\frac{1}{4} & -3b \\ -3b & c & -3b & -\frac{1}{4} \\ -\frac{1}{4} & -3b & c & -3b \\ -3b & -\frac{1}{4} & -3b & c \end{Bmatrix}. \quad (37)$$

Based on relation (20), we have from (37)

$$\mathcal{B}_\Delta^{(3)} = \begin{Bmatrix} c + 3b & 0 & 3b - \frac{1}{4} \\ \frac{1}{4} - 3b & c + \frac{1}{4} & \frac{1}{4} - 3b \\ 3b - \frac{1}{4} & 0 & c + 3b \end{Bmatrix}. \quad (38)$$

Two types of antivibrational motion should be considered here.

(i) Pairwise out-of-phase (asynchronous) motion, as shown in Fig. 4a, with the constraints

$$\Delta_1 = -\Delta_3, \quad \Delta_2 = -\Delta_4, \quad \Delta_2 = -\Delta_1. \quad (39)$$

(ii) Pairwise in-phase (synchronous) (anti)vibration, Fig. 4b,

$$\Delta_1 = \Delta_3, \quad \Delta_2 = \Delta_4, \quad \Delta_2 = -\Delta_1. \quad (40)$$

With the help of Eqs. (20) and (40) the matrix (38) is reduced to the single element

$$\lambda_{syn}^{(\Delta)} \equiv \lambda_{\Delta}^{(+)} = c - \frac{1}{4} + 6b = 2Q + \frac{1}{2}(\sqrt{2} - 1). \quad (41)$$

Similarly, we obtain for the asynchronous mode

$$\lambda_{asyn}^{(\Delta)} \equiv \lambda_{\Delta}^{(-)} = 2Q - \frac{\sqrt{2}}{4}. \quad (42)$$

Hence, the short-term behaviour equations of motion are

$$\Delta^{(+)} = \alpha_1 e^{\omega_{\Delta}^{(+)} t} + \alpha_2 e^{-\omega_{\Delta}^{(+)} t}, \quad (43)$$

$$\Delta^{(-)} = \beta_1 e^{\omega_{\Delta}^{(-)} t} + \beta_2 e^{-\omega_{\Delta}^{(-)} t}, \quad (44)$$

where α, β are arbitrary constants and

$$\omega_{\Delta}^{(+,-)} = \frac{\sqrt{\lambda_{\Delta}^{(+,-)}}}{r_L^{3/2}}. \quad (45)$$

Lyapunov exponent λ_r is given by the maximum value

$$\lambda_r = \max[\omega_{\Delta}^{(+,-)}], \quad (46)$$

where the instability exponents are given explicitly by

$$\omega_{\Delta}^{(+)} = \frac{\eta_{\Delta}^{(+)}}{(2L+1)^3}, \quad (47)$$

$$\eta_{\Delta}^{(+)} = 512 \sqrt{2Q + \frac{1}{2}(\sqrt{2} - 1)} \left(Q - \frac{1}{4} - \frac{1}{\sqrt{2}} \right)^{3/2}, \quad (48)$$

and

$$\omega_{\Delta}^{(-)} = \frac{\eta_{\Delta}^{(-)}}{(2L+1)^3}, \quad (49)$$

$$\eta_{\Delta}^{(-)} = 512 \sqrt{2Q - \frac{\sqrt{2}}{4}} \left(Q - \frac{1}{4} - \frac{1}{\sqrt{2}} \right)^{3/2}. \quad (50)$$

The instability (Lyapunov) exponent $\omega_{\Delta}^{(+)}$, as given by (47), governs the lifetime of the excited state. It corresponds to the case when two neighbouring electrons start falling to the centre, while the other two are escaping at their expense. In the synchronous case two opposing electrons recede from the nucleus, at the expense of the other two falling inwards, as illustrated in Fig. 4. Note, however, that neither of the equations used here governs the long-term system behaviour, since we are all the time within the first order perturbation (small deviations) theory.

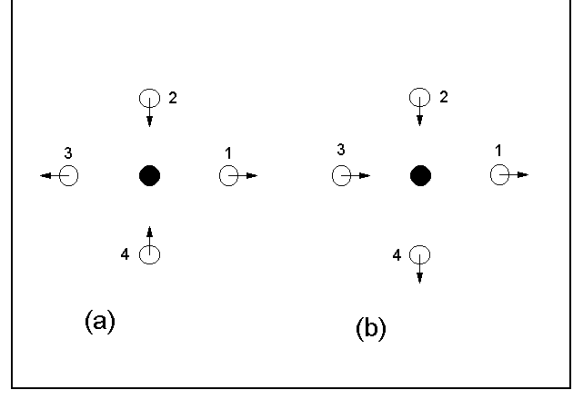


Fig. 4. Antivibrational modes along the radial motion.

3.3. Out-of-plane deviations

As in the previous case, through-the-plane oscillations possess two different modes, shown in Fig. 5. In order to evaluate the corresponding frequencies we start from (15).

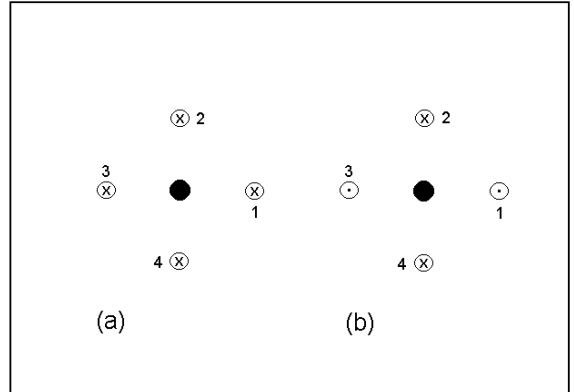


Fig. 5. Two vibration modes for the out-of-plane oscillations. In-phase and out-of-phase oscillations are denoted by the crosses and dots, respectively.

Substituting (15) into (10) one obtains for ∇_1

$$r^3 \frac{d^2 \nabla_1}{dt^2} = \left(\frac{1}{8} + \frac{1}{\sqrt{2}} - Q \right) \nabla_1 - \frac{1}{\sqrt{8}} \nabla_2 - \frac{1}{8} \nabla_3 - \frac{1}{\sqrt{8}} \nabla_4. \quad (51)$$

Similarly for the other three electrons (see Appendix) and after accounting for the constraints (17) we arrive at the equation

$$r^3 \frac{d^2}{dt^2} \left\{ \begin{array}{c} \nabla_1 \\ \nabla_2 \end{array} \right\} = \mathcal{N}_{\nabla} \left\{ \begin{array}{c} \nabla_1 \\ \nabla_2 \end{array} \right\}, \quad (52)$$

where the matrix in the restricted space is

$$\mathcal{N}_{\nabla} = \left\{ \begin{array}{cc} \frac{1}{\sqrt{2}} - Q & -\frac{1}{\sqrt{2}} \\ -\frac{1}{\sqrt{2}} & \frac{1}{\sqrt{2}} - Q \end{array} \right\}. \quad (53)$$

Solving the corresponding secular equation (see Appendix), one has for the eigenvalues

$$\lambda_{\nabla}^{(+,-)} = \frac{1}{\sqrt{2}} - Q \pm \frac{1}{\sqrt{2}}. \quad (54)$$

The first root corresponds to the pairwise $\nabla_1 = \nabla_3 = -\nabla_2 = -\nabla_4$ and the second to the all four electrons $\nabla_1 = \nabla_3 = \nabla_2 = \nabla_4$ in-phase oscillations respectively, as shown in Figs. 5a and 5b.

From the relation analogous to (34)

$$\omega_{\nabla}^{(+,-)} = \frac{\sqrt{-\lambda_{\nabla}^{(+,-)}}}{r_L^{3/2}}, \quad (55)$$

and (54) we have

$$\omega_{\nabla}^{(+,-)} = \frac{\eta_{\nabla}^{(+,-)}}{(2L+1)^3}, \quad (56)$$

$$\eta_{\nabla}^{(+,-)} = 512 \sqrt{Q - \frac{1}{\sqrt{2}} \pm \frac{1}{\sqrt{2}} \left(Q - \frac{1}{4} - \frac{1}{\sqrt{2}} \right)^{3/2}}. \quad (57)$$

3.4. Vibronic spectra

Vibronic modes are excited for sufficiently large ρ_L . To locate thresholds for vibronic modes appearance, we make use of the classical oscillator energy in order to estimate the amplitude of the harmonic oscillations (see Grujić 1999). If the energy of the oscillator is evaluated both classically and quantum mechanically, namely

$$E_{\text{class}} = \frac{1}{2} \omega^2 a^2, \quad (58)$$

$$E_{\text{quant}} = \left(m + \frac{1}{2} \right) \omega, \quad m = 0, 1, 2, \dots, \quad (59)$$

one has, for $a \ll \rho_L$ (see (15)),

$$2L + 1 \gg \gg 6 \sqrt{\frac{-Q_{\text{eff}}}{\lambda}} (2m + 1), \quad m = 0, 1, 2, \dots, \quad (60)$$

where $\gg \gg$ implies, somewhat arbitrarily, the factor 25. Here we include zero-field (purely quantum mechanical) energy ($m=0$). Substituting (34) into (59) we have for the i -th vibrational mode

$$E_{\text{vib}}^{(i)} = \left(m_i + \frac{1}{2} \right) \frac{\sqrt{-\lambda_i}}{r_L^{3/2}}, \quad m_i = 0, 1, 2, \dots \quad (61)$$

In order to compare the magnitude of rotational and vibrational energies, we evaluate the ratio

$$\frac{E_{\text{vib}}^{(i)}}{|E_L^{(0)}|} = \kappa \frac{2m + 1}{2L + 1}, \quad (62)$$

where

$$\kappa = \frac{32}{27} \sqrt{\frac{-\lambda}{Q_{\text{eff}}}}. \quad (63)$$

Hence, accounting for the limitation of m range by (60), relative contributions from the vibrational degrees of freedom remain finite as the orbital mode excitations increase.

Since the energy gaps between adjacent rotational levels decrease with L , it is of interest to see how this energy difference compares with the vibrational mode energies. From (13) we have

$$\begin{aligned} \Delta E_{L+1,L} &\equiv E_{L+1} - E_L \\ &= 576 Q_{\text{eff}}^2 \frac{L + 1}{[(2L + 1)(2L + 3)]^2} \\ &\sim \frac{36 Q_{\text{eff}}^2}{L^3}. \end{aligned} \quad (64)$$

On the other hand we have from (61)

$$E_{\text{vib}}^{(i)} \sim \gamma \frac{m_i + \frac{1}{2}}{L^3}, \quad m_i < m_i^{(\text{max})}, \quad \gamma = \frac{64 Q_{\text{eff}}}{3}, \quad (65)$$

where $m_i^{(\text{max})}$ is the maximum m_i allowed by (60). Comparing (61) and (65), we see that a mere increase of rotational excitation degree does not lead to an overlap of energy levels with different L -s.

4. NUMERICAL RESULTS - BERYLLIUM (P1 MODEL)

We calculate rovibronic spectra for the neutral atomic system. Since within our first-order approximation in-plane and out-of-plane motion decouple, we treat both kinematics separately.

Matrix $\mathcal{B}^{(8)}$ from (23) for $Q = 4$ reads

$$\mathcal{B}^{(8)} = \begin{pmatrix} -4.2285 & 0.53034 & 0.25 & 0.53034 & 0 & 0.17678 & 0 & 0.17678 \\ 0.53034 & -4.2285 & 0.53034 & 0.250 & 0.17678 & 0 & 0.17678 & 0 \\ 0.25 & 0.53034 & -4.2285 & 0.53034 & 0 & -0.17678 & 0 & 0.17678 \\ 0.53034 & 0.25 & 0.53034 & -4.2285 & 0.17678 & 0 & -0.17678 & 0 \\ 0 & 0.17678 & 0 & -0.17678 & 7.39645 & -0.53034 & -0.25 & -0.53034 \\ -0.17638 & 0 & 0.17678 & 0 & -0.53034 & 7.39645 & -0.53034 & -0.25 \\ 0 & -0.17678 & 0 & 0.17678 & -0.25 & 0.53034 & 7.3964 & -0.53034 \\ 0.17678 & 0 & -0.17678 & 0 & -0.53034 & -0.25 & -0.53034 & 7.3964 \end{pmatrix}. \quad (66)$$

We notice that the diagonal elements in (66) appear much larger than the off-diagonal ones. In particular, elements coupling δ and Δ subspaces are small. As a consequence of the mutual couplings, all deviations share both stable (oscillatory) and unstable (exponentially decaying) modes. It is the \mathcal{U} matrix elements that determine the share of these modes for each small deviation, as can be seen from Eq. (21).

From (30) we have

$$\omega_{\delta}^{(0)} = \frac{6175.92}{(2L+1)^{3/2}}, \quad (67)$$

and from (35)

$$\omega_{\delta}^{(-)} = \frac{5669.94}{(2L+1)^{3/2}}, \quad (68)$$

with both frequencies close to each other, $\omega_{\delta}^{(-)}/\omega_{\delta}^{(0)} = 0.91807$. Similarly, from (56)

$$\omega_{\nabla}^{(+)} = \frac{3231.13}{(2L+1)^{3/2}}, \quad (69)$$

$$\omega_{\nabla}^{(-)} = \frac{2597.82}{(2L+1)^{3/2}}, \quad (70)$$

with ratio $\omega_{\nabla}^{(-)}/\omega_{\nabla}^{(+)} = 0.8040$. From (47) and (49) we have

$$\omega_{\Delta}^{(+)} = \frac{4628.27}{(2L+1)^{3/2}}, \quad (71)$$

$$\omega_{\Delta}^{(-)} = \frac{3555.58}{(2L+1)^{3/2}}, \quad (72)$$

that gives $\omega_{\Delta}^{(-)}/\omega_{\Delta}^{(+)} = 0.7682$.

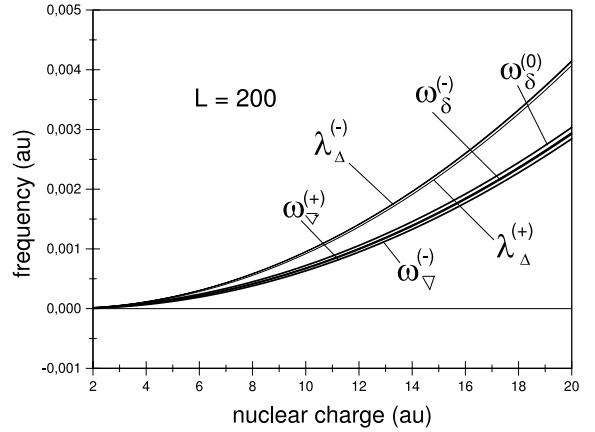


Fig. 6. Vibrational frequencies $\omega_{\delta}, \omega_{\nabla}$ and anti-vibrational frequency λ_{Δ} (Lyapunov exponent) vs. nuclear charge.

We plot ω values versus the nuclear charge in Fig. 6. Note the closeness of $\omega_{\delta}^{(0)}$ (denoted by ω_{δ} in Fig. 6) and $\omega_{\delta}^{(-)}$. The increase of the related frequencies with Q indicates the growing "stiffness" of the system as the strength of the nuclear field rises. On the other hand, the frequency ratio is L -independent. From (60) one has the condition for the onset of the corresponding harmonic vibrations

$$2L_{1,2}^{(\min)} + 1 \gg \gg 6 \sqrt{\frac{-Q_{\text{eff}}}{\lambda_{1,2}}} (2m_{1,2} + 1). \quad (73)$$

Minimum L_{max} values for exciting vibrational modes are given in Table 1, together with the corresponding stability indices ν

$$\nu = \omega T = 2\pi \sqrt{\frac{\lambda}{Q_{\text{eff}}}} = 2\pi \frac{T}{\tau_{\omega}}, \quad (74)$$

where τ_{ω} is the vibrational period and T is the system rotational period. Numerical results indicate that the system is highly unstable, what appears to be a common feature of the regular structures based on the correlation effects.

Table 1. Some parameters for the quadruply excited system. L_{\min} is the minimum L for excitation of a particular vibrational mode; ν is the stability index for the particular mode (see text).

	L_{\min}			ν
	$m = 0$	$m = 1$	$m = 2$	
$\delta^{(-)}$	40	120	200	7.5155
$\delta^{(0)}$	58	173	287	8.186
$\nabla^{(+)}$	66	197	327	7.203
$\nabla^{(-)}$	82	244	407	5.792

In view of the rather vague nature of (73) requirement, the estimate of a threshold for the onset of the corresponding vibrational motion appears somewhat arbitrary.¹

We show in Table 2 a number of relevant quantities for the quadruply excited beryllium atom, where r_{eq} is the radius of the equilibrium system orbit, λ_r is the Lyapunov exponent and τ is the level lifetime

$$\tau = \frac{\ln 2}{\lambda_r}. \quad (75)$$

Table 2. Semiclassical system parameters for the quadruply excited four-electron system with $Q = 4$. All quantities are in atomic units. In parentheses the power of 10 is given by which the number is to be multiplied. L_{\max} is the maximum system angular momentum quantum number, r_{eq} the single electron equilibrium distance, λ_r is Lyapunov exponent, τ is the lifetime, T is the rotational period, (see text).

L_{\max}	r_{eq}	λ_r	τ	T
10	2.2645	9.423(-1)	7.356(-1)	1.2274(1)
25	13.356	6.579(-2)	1.054(1)	1.758(2)
40	3.369(1)	1.642(-2)	4.221(1)	7.043(2)
58	7.029(1)	5.449(-3)	1.272(2)	2.123(3)
66	9.083(1)	3.709(-3)	1.869(2)	3.118(3)
82	1.398(2)	1.942(-3)	3.569(2)	5.954(3)
120	2.982(2)	6.234(-4)	1.112(3)	1.855(4)
173	6.183(2)	2.088(-4)	3.32(3)	5.538(4)
197	8.012(2)	1.416(-4)	4.895(3)	8.169(4)
200	8.257(2)	1.353(-4)	5.123(3)	8.546(4)

Numerical results for the rovibronic spectrum are given in Table 3.

The spectrum appears much more complex than that of the triple excited system, like the one from (Grujić 1999). Each of the two independent degrees of freedom (in- and out-of-plane motions) has two different modes of vibrational kinematics. Within a particular degree of freedom different modes alternate, i.e. they can not coexist. On the contrary, a particular mode from an out-of-plane motion couples with a mode from an in-plane degree of freedom.

Strictly speaking, the zero energies ($m = 0$) do not belong to the semiclassical theory, but are included more for the sake of completeness and comparison, as it was done in the previous calculations (Grujić 1999). As can be seen from Table 3, vibrational excitations raise the energy levels by noticeable amounts. This is more evident in Fig. 7, where rovibrational energy levels are plotted in the form of a histogram. The first column is in fact absent from the model, but is presented for the sake of comparison. As the degree of excitation of the basic levels raises, higher vibrational levels appear and the vibrational modes become more prominent. Hence, the model moves the energy diagram further away from the rotor-like ansatz, where vibrational modes dominate and rotational degree contributions appear as small superpositions to the basic vibrational energies, as is the case with molecules. It shows *a posteriori* that the rigid-rotator picture is inadequate for describing rovibrational structure of the Coulombic systems, as argued above.

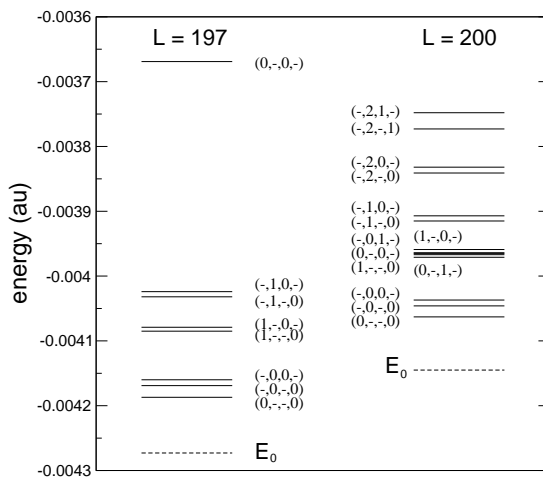


Fig. 7. Rovibrational energies for $L = 197, 200$. Vibrational quantum numbers $m_{\delta}^{(-)}$, $m_{\delta}^{(0)}$, $m_{\nabla}^{(+)}$, $m_{\nabla}^{(-)}$ are denoted (see Table 3).

¹Another choice would be to take straightway diagonal elements of (53), before further manipulating the vibrational matrix, what would correspond to the zero-order approximation; thus, for $m = 1$ one would obtain $L_1^{(\min)} \approx 200$, and similarly $L_2^{(0)} \approx 350$ for $m = 2$.

Table 3. Rovibronic spectrum for Be. All quantities are in atomic units. L_{\max} is the system maximum angular momentum quantum number, E_0 is the zero-order system energy, ω and m are the vibrational angular frequencies and quantum numbers, respectively, and E_{tot} is the system total energy. In parentheses the power of 10 is given by which the number is to be multiplied.

L_{\max}	$-E_0$	$\omega_{\delta}^{(0)}$	$\omega_{\delta}^{(-)}$	$\omega_{\nabla}^{(+)}$	$\omega_{\nabla}^{(-)}$	$m_{\delta}^{(0)}$	$m_{\delta}^{(-)}$	$m_{\nabla}^{(+)}$	$m_{\nabla}^{(-)}$	$-E_{tot}$
10	1.5117(0)	-	-	-	-	-	-	-	-	1.5117(0)
25	2.563(-1)	-	-	-	-	-	-	-	-	2.563(-1)
39	1.068(-1)	-	-	-	-	-	-	-	-	1.068(-1)
40	1.016(-1)	-	1.587(-2)	-	-	-	0	-	-	9.366(-2)
58	4.870(-2)	-	5.266(-3)	-	-	-	0	-	-	4.607(-2)
58	4.870(-2)	3.856(-3)	-	-	-	0	-	-	-	4.677(-2)
66	3.769(-2)	-	3.584(-3)	2.310(-3)	-	-	0	0	-	3.463(-2)
66	3.769(-2)	2.625(-3)	-	2.310(-3)	-	0	-	0	-	3.434(-2)
82	2.449(-2)	1.375(-3)	-	1.210(-3)	-	0	-	0	-	2.295(-2)
82	2.449(-2)	-	1.868(-3)	1.210(-3)	-	-	0	0	-	2.289(-2)
82	2.449(-2)	1.375(-3)	-	-	9.728(-4)	0	-	-	0	2.331(-2)
82	2.449(-2)	-	1.868(-3)	-	9.728(-4)	-	0	-	0	2.307(-2)
120	1.148(-2)	4.412(-4)	-	3.883(-4)	-	0	-	0	-	1.106(-2)
120	1.148(-2)	4.412(-4)	-	-	3.122(-4)	0	-	-	0	1.110(-2)
120	1.148(-2)	-	6.0257(-4)	3.883(-4)	-	-	0	0	-	1.098(-2)
120	1.148(-2)	-	6.0257(-4)	-	3.122(-4)	-	0	-	0	1.101(-2)
120	1.148(-2)	-	6.0257(-4)	-	3.122(-4)	-	1	-	0	1.042(-2)
120	1.148(-2)	-	6.0257(-4)	3.883(-4)	-	-	1	0	-	1.038(-2)
173	5.537(-3)	-	2.0189(-4)	1.301(-4)	-	-	0	0	-	5.371(-3)
173	5.537(-3)	1.478(-4)	-	1.301(-4)	-	0	-	0	-	5.398(-3)
173	5.537(-3)	1.478(-4)	-	-	1.046(-4)	0	-	-	0	5.411(-3)
173	5.537(-3)	-	2.0189(-4)	-	1.046(-4)	-	0	-	0	5.384(-3)
173	5.537(-3)	-	2.0189(-4)	1.301(-4)	-	-	1	0	-	5.156(-3)
173	5.537(-3)	-	2.0189(-4)	-	1.046(-4)	-	1	-	0	5.171(-3)
173	5.537(-3)	1.478(-4)	-	1.301(-4)	-	1	-	0	-	5.250(-3)
173	5.537(-3)	1.478(-4)	-	-	1.046(-4)	1	-	-	0	5.263(-3)
197	4.273(-3)	-	1.3685(-4)	8.819(-5)	-	-	0	0	-	4.160(-3)
197	4.273(-3)	1.002(-4)	-	8.819(-5)	-	0	-	0	-	3.669(-3)
197	4.273(-3)	1.002(-4)	-	-	7.091(-5)	0	-	-	0	4.187(-3)
197	4.273(-3)	-	1.3685(-4)	-	7.091(-5)	-	0	-	0	4.169(-3)
197	4.273(-3)	-	1.3685(-4)	8.819(-5)	-	-	1	0	-	4.024(-3)
197	4.273(-3)	-	1.3685(-4)	-	7.091(-5)	-	1	-	0	4.032(-3)
197	4.273(-3)	1.002(-4)	-	8.819(-5)	-	1	-	0	-	4.079(-3)
197	4.273(-3)	1.002(-4)	-	-	7.091(-5)	1	-	-	0	4.085(-3)
200	4.145(-3)	-	1.3083(-4)	8.429(-5)	-	-	0	0	-	4.037(-3)
200	4.145(-3)	-	1.3083(-4)	-	6.777(-5)	-	0	-	0	4.046(-3)
200	4.145(-3)	9.578(-5)	-	8.429(-5)	-	0	-	0	-	3.965(-3)
200	4.145(-3)	9.578(-5)	-	-	6.777(-5)	0	-	-	0	4.063(-3)
200	4.145(-3)	-	1.3083(-4)	8.429(-5)	-	-	1	0	-	3.907(-3)
200	4.145(-3)	-	1.3083(-4)	-	6.777(-5)	-	1	-	0	3.915(-3)
200	4.145(-3)	9.578(-5)	-	8.429(-5)	-	1	-	0	-	3.959(-3)
200	4.145(-3)	9.578(-5)	-	-	6.777(-5)	1	-	-	0	3.967(-3)
200	4.145(-3)	9.578(-5)	-	8.429(-5)	-	0	-	1	-	3.971(-3)
200	4.145(-3)	-	1.3083(-4)	8.429(-5)	-	-	0	1	-	3.964(-3)
200	4.145(-3)	-	1.3083(-4)	-	6.777(-5)	-	2	-	0	3.841(-3)
200	4.145(-3)	-	1.3083(-4)	8.429(-5)	-	-	2	0	-	3.832(-3)
200	4.145(-3)	-	1.3083(-4)	8.429(-5)	-	-	2	1	-	3.748(-3)
200	4.145(-3)	-	1.3083(-4)	-	6.777(-5)	-	2	-	1	3.773(-3)

5. DISCUSSION AND CONCLUSIONS

The extension from the triply to quadruply excited states turns out nontrivial. First, the number of possible underlying classical configurations raises considerably. We have restricted ourselves in this paper to one of the most simple planar models, but even in this case the spectrum appears very complex. Even when neglecting coupling between vibrational modes and rotational motion, as well as those between different vibrational modes themselves, calculations become cumbersome.

At present, the principal results and the respective conclusions appear more of a heuristic than practical value, displaying the complexity of the physical behaviour of the few-electron systems. Even if feasible from the experimental point of view, such highly multiply excited systems would hardly provide distinctive line spectra. Rather, they would be better interpreted in terms of statistical approach, than by regular semiclassical behaviour.

Four equivalent electrons obviously violate Pauli's principle, but in real highly excited states two pairs of equivalent electrons are practically indistinguishable from the four intrashell particles. One may consider the system as composed of two equivalent electrons with opposite spins and with $L = L_{\max}/2$, and another pair with $L = (L_{\max} - 1)/2$, both practically with circular, mutually indistinguishable orbits.

If the present results are to be compared with the relevant quantum mechanical ones, that in the absence of experimental data appears to be the only criterion for judging of the procedure employed, one must bear in mind that the two approaches are complementary. First, full quantum mechanical calculations are still feasible for the low-lying states only, where the semiclassical approach is not expected to work. Second, the restricted model calculations, like those within the frozen- r approximation, are still of qualitative nature, aiming mainly at classifying possible quantum states. In this respect, semiclassical modeling can be helpful in choosing underlying configurations that may be used for the quantum mechanical calculations. How much effective this approach can be is well illustrated by the theory of near-threshold fragmentation, which has been based on the purely classical model by Wannier.

Generally, highly excited states belong to the domain of correspondence principle and can serve as tools for elucidating many quantum mechanical features of the atomic systems via a more transparent semiclassical models. Calculations presented in this paper should hopefully contribute to this end. In this respect further studies of relevant classical configurations, like that of tetrahedron type as sketched at the beginning of the present paper, would be desirable.

Acknowledgements – This work has been supported by the Ministry of Science of Serbia, through project No 101429.

REFERENCES

Bao, C.G.: 1992, *J. Phys. B*, **25**, 3725.
 Bao, C.G.: 1993, *Phys. Rev.*, **A47**, 1752.
 Bao, C.G.: 1998, *Phys. Lett.*, **A 250**, 123.
 Bao, C.G. and Duan Y.: 1994, *Phys. Rev.*, **A49**, 818.
 Cvejanović, S, Dohčević, Z.D., Grujić, P.: 1990, *J. Phys. B*, **23**, L167.
 Grujić, P.: 1983, *J. Phys.*, **B16**, 2567.
 Grujić, P.: 1988, *J. Phys. B*, **21**, 63.
 Grujić, P.: 1999, *Eur. Phys. J.*, **D6**, 441.
 Hasegawa, S., Yoshida, S.F., Matsuoka, L., Koike, F., Fritzsche, S., Obara, S., Azuma, Y. and Nagata, T.: 2006, *Phys. Rev. Lett.*, **97** 023001.
 Komninou, Y. and Nicolaides, C.: 1994, *Phys. Rev.*, **A50**, 3782.
 Kuchiev, Y., Ostrovsky, V.: 1998, *Phys. Rev.*, **A58**, 321.
 Landau, L. and E. Lifshitz, E.: 1965, *Quantum Mechanics* (Pergamon Press, Oxford).
 Madsen, L.B.: 2003, *J. Phys. B*, **36**, R223.
 Madsen, L.B. and Molmer, K.: 2001, *Phys. Rev.*, **A64**, 060501(R).
 Madsen, L.B. and Molmer, K.: 2002, *Phys. Rev.*, **A65**, 022506.
 Morishita, T. and Lin, C.D.: 2005, *Phys. Rev.*, **A71**, 012504.
 Nicolaides, C., Pianos, N., Komninou, Y.: 1993, *Phys. Rev.*, **A48**, 3578.
 Poulsen, M. and Madsen, P.: 2005, *Phys. Rev.*, **A71**, 062502.
 Poulsen, M. and Madsen, P.: 2005, *Phys. Rev.*, **A72**, 042501.
 Simonović, N. and Grujić, P.: 2007, *Eur. Phys. J. D*, **42**, 1.
 Simonović, N. and Grujić, P.: 1996, in *Adv. Math. Study Atom. Doubly-Exc. States*, Medellin, Colombia, 1995. Eds. J. Mahecha, J. Botero, Universidad de Antioquia, pp. 107-53.
 Walter, M., Briggs, J.S. and Feagin, J.M.: 2000, *J. Phys. B*, **33**, 2907.
 Wannier, G.H.: 1953, *Phys. Rev.*, **90**, 817.

APPENDIX

We rewrite (51) as

$$D^2 \nabla_1 = f_1(\nabla), \tag{76}$$

where ∇ denotes the set $(\nabla_1, \nabla_2, \nabla_3, \nabla_4)$. From the cycling symmetry of the system, one has

$$\begin{aligned} D^2 \nabla_2 &= f_1(\nabla_1 \rightarrow \nabla_2, \nabla_2 \rightarrow \nabla_3, \\ &\nabla_3 \rightarrow \nabla_4, \nabla_4 \rightarrow \nabla_1) \equiv f_2, \end{aligned} \tag{77}$$

$$\begin{aligned} D^2\nabla_3 &= f_2(\nabla_2 \rightarrow \nabla_3, \nabla_3 \rightarrow \nabla_4, \\ &\nabla_4 \rightarrow \nabla_1, \nabla_1 \rightarrow \nabla_2) \equiv f_3, \end{aligned} \quad (78)$$

$$\begin{aligned} D^2\nabla_4 &= f_3(\nabla_3 \rightarrow \nabla_4, \nabla_4 \rightarrow \nabla_1, \\ &\nabla_1 \rightarrow \nabla_2, \nabla_2 \rightarrow \nabla_3) \equiv f_4. \end{aligned} \quad (79)$$

The system (76)-(79) can be rewritten in the matrix form as

$$D^2H = \mathcal{F}H, \quad (80)$$

where H is the corresponding column vector and

$$\mathcal{F} = \begin{Bmatrix} a' & b' & -b'^2 & b' \\ b' & a' & b' & -b'^2 \\ -b'^2 & b' & a' & b' \\ b' & -b'^2 & b' & a' \end{Bmatrix}, \quad (81)$$

where $a' = \frac{1}{8}(1 + 4\sqrt{2}) - Q$ and, $b' = -\frac{1}{\sqrt{8}}$.

Imposing the condition $L_x = 0$, $L_y = 0$, one has respectively

$$\nabla_2 = \nabla_4, \quad \nabla_1 = \nabla_3, \quad (82)$$

what gives (52) and (53) in the text. Requiring

$$\det[\mathcal{N}_r - \mathcal{I}\lambda] = 0, \quad (83)$$

one obtains the eigenvalues (54).

СЕМИКЛАСИЧНА ИЗРАЧУНАВАЊА ЧЕТВОРОСТРУКО ПОВУЂЕНИХ ЧЕТВОРОЕЛЕКТРОНСКИХ СИСТЕМА

N. Simonović¹, M. Predojević², V. Panković² and P. Grujić¹

¹*Institute of Physics, P.O. Box 57, 11000 Belgrade, Serbia*

²*Gymnasium, Trg Pobede 2a, 22320 Indjija, Serbia*

УДК 52-472

Оригинални научни рад

Високо побуђени атоми попримају врло велике димензије и могу се наћи само у веома разређеном гасном стању, попут оног у међузвезданом простору. Вишеструко побуђени системи попут берилијума, ексцитирани до великих главних квантних бројева, имају радијус $r \sim 10 \mu$. Изучаван је семикласични спектар четвороструко високопобуђених четвороелектронских атомских система за случај раванског модела еквивалентних електрона. Енергија система састоји се од ротационих и вибрационих мода у оквиру

приближно кружне електронске орбите, као што је рађено у претходним израчунавањима за троструко побуђене троелектронске системе. Овде презентирамо нумеричке резултате за атом берилијума. Полуживоти семикласичних стања процењени су помоћу одговарајућих Љапуновљевих експонената. Релативни доприноси вибрационих мода енергијским нивоима расту са степеном кулонских побуђивања. Значај добијених резултата дискутован је како са опсервационе, тако и еуристичке тачке гледишта.